Chapter 25

AFM, STM AND STS STUDIES OF GRAIN BOUNDARIES AND ION-BEAM INDUCED DEFECTS IN MgB_2

A V. Narlikar [a,b] , P.S.P. Herrmann[c] , S.B. Samanta[a] , H. Narayan[a], Anurag Gupta[a], D. Kanjilal[d], R. Vijayaraghavan[e], T. Muranaka[f] and J. Akimitsu[f]

(a) *National Physical Laboratory, Dr. K.S. Krishnan Marg, New Delhi 110 012, INDIA.*
(b) *Departamento de Fisica, UFSCAR, São Carlos, BRAZIL.*
(c) *EMBRAPA – CNPDIA, Sao Carlos, BRAZIL.*
(d) *Nuclear Science Centre, PO Box 10502, Aruna Asaf Ali Marg, New Delhi 110 067, INDIA.*
(e) *Tata Institute of Fundamental Research, Mumbai 400 005, INDIA.*
(f) *Department of Physics, Aoyama-Gakuin University, 6-16-1 Chitosedai, Setagaya-ku, Tokyo, 157-8572, JAPAN.*

(*Received on 21 June, 2001*)

1. INTRODUCTION

Recent discovery [1] of superconducting magnesium diboride (MgB_2) with an unexpected high superconducting critical temperature T_c of 39K has led to an enormous excitement in experimental and theoretical research on this new binary intermetallic compound. Some of the exciting macroscopic features that the initial experiments revealed were the anisotropic nature [2] of the material (although the anisotropy factor was much less than in HTS cuprates), lack of the grain boundary weak link effect and a potential to realise appreciable J_c values in high magnetic field [3-5]. On the microscopic front, several experiments like Boron isotope effect [6,7], the specific heat [8,9], pressure dependence of T_c [10] and NMR [11] seem to support an active involvement of phonons in mediating superconducting pairs, as in any conventional low T_c superconductor. The energy gap coefficient estimated from some of the above experiments as well as from tunnelling studies [12] however seems to suggest the electron-phonon coupling to vary from rather weak to strong. More recent experimental data (see articles in the present volume) indicate the existence of two energy gaps. On the

Superconducting Magnesium Diboride
(*Studies of High Temperature Superconductors Volume 38*)
Ed.: Anant Narlikar, Nova Science Publishers, New York.
ISBN: 1-59033-131-1

other hand, MgB_2 has several features common with the HTS cuprates [13] and some properties like Hall Effect and thermal conductivity are found different from the conventional low T_c superconductors. The band structure of the material is more complex [14-16] and is semi-metal like, which is believed to be responsible for the unusual superconducting properties. Concerning the basic microscopic mechanism responsible for high T_c of MgB_2, which is yet to be resolved, the observed experimental data are being largely discussed in two fundamentally different frameworks: the BCS electron-phonon mechanism [14] and various approaches based on coulomb interactions [17-19], which are claimed to yield, directly or indirectly, high T_c superconductivity. Also, the possible contribution of the resonating valence bonds (RVB) to the superconductivity of MgB_2 has been suggested [20].

This short chapter briefly consolidates some of our work on MgB_2 focusing on an important macroscopic issue of topical interest. In particular we address the question, why the grain boundaries in polycrystalline MgB_2 are indeed so indifferent to cause the weak-link effects? We attempt to find an answer through high-resolution studies – extending down to the atomic resolution by using AFM, STM and STS techniques. Although the main theme of this chapter relates to MgB_2, we compare the situation with another intermetallic, namely polycrystalline YNi_2B_2C, a quaternary borocarbide, with a lower T_c of 15.5 K, but its natural grain boundaries are reported to exhibit the weak link effect. For comparision we present a high resolution STM/STS study of grain boundaries also in this material. We finally take a hurried look at the atomically resolved images of the basal plane of the unit cell of MgB_2 and present the images of defect tracks produced by the ion beam irradiation. The possible importance of these extended defects in the current transport is briefly discussed.

2. MATERIAL SYNTHESIS AND GRAIN MORPHOLOGY

The MgB_2 samples investigated in the present study were synthesized at the Department of Physics, Aoyama – Gakuin University, Japan, as described in detail elsewhere [1]. Accordingly, the sintered samples revealed a sharp superconducting transition, measured both resistively and inductively, at 39 K. The characteristic crystal structure, corresponding to the space group P6/mmm, with the lattice parameters of a = 0.3086 nm and c = 0.3524 nm was confirmed using the room temperature XRD.

The polycrystalline sample of quarternary borocarbide, YNi_2B_2C, which has been presently studied in conjunction with MgB_2 was synthesized at the Tata Institute of Fundamental Research, Mumbai by conventional arc melting technique. It was phase pure as confirmed by XRD and showed a sharp transition both resistively and inductively at 15.5 K.

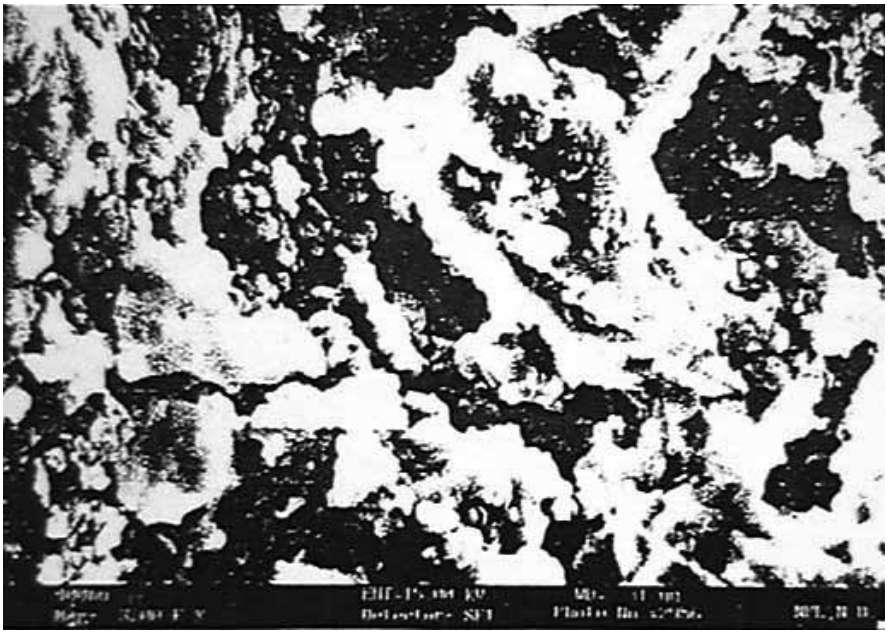

Fig. 1: SEM image showing grain-structure of the sintered sample.

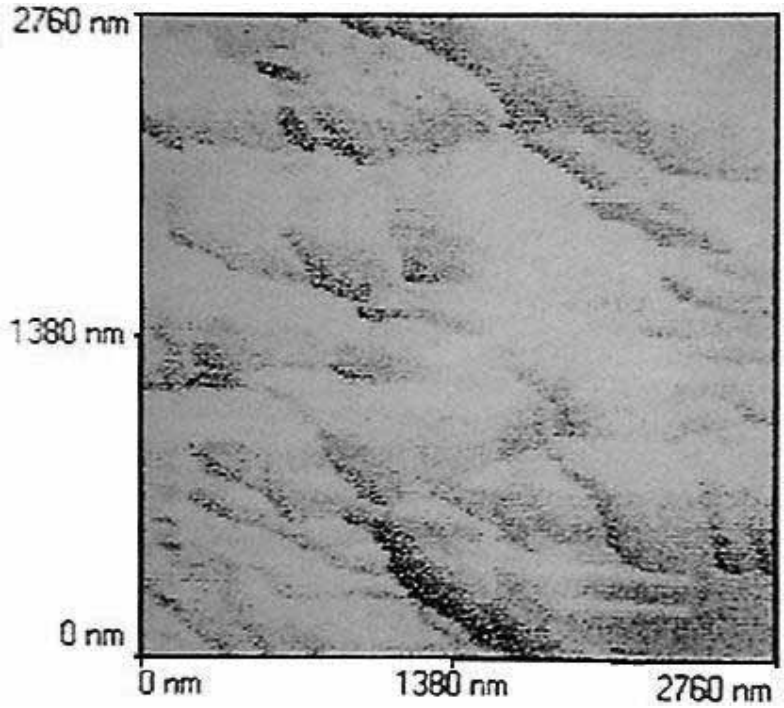

Fig. 2: AFM image showing the presence of small equiaxed grains.

Fig.1 shows a typical SEM image of the sintered MgB_2 sample, which depicts a wide variation of the grain size. However, small grains of size 200 to 400 nm diameter, which seem to constitute larger grains, are in abundance. Moreover, these small grains are essentially found equiaxed or spherical in shape and thus they are unlikely to be the cause of anisotropy in the macroscopic transport properties. The SEM image of Fig.1 also shows the presence of voids, as generally found in a sintered sample. The possibility of unidentified MgO as an impurity phase is not ruled out.

The sub-micron grain size observed by SEM is further corroborated from AFM studies carried out in the contact mode. A typical image depicting a very small grain-size is presented in Fig.2. Our AFM observations revealed (Fig.3a) some of the grains had the characteristic hexagonal form with well developed faces as observed in carefully grown bulk single crystals. Fig.3b shows a zoomed image of one such grain having well developed faces located at a different region of the sample.

3. STM/STS STUDIES OF GRAIN BOUNDARIES – Why no weak link effect?

One of the important features of MgB_2 is that the natural grain boundaries in its polycrystalline sample [3] do not, or only marginally exhibit the weak link effects. This is technologically extremely important because unlike in high T_c cuprates [21], where the critical current density J_c of the conductor is markedly reduced by grain boundaries serving as weak links, MgB_2 possesses a relatively large coherence length (around 4 nm to 5 nm), exceeding the supposedly narrow grain boundary width. Consequently, the neighbouring grains of the material are no longer weakly coupled to favour Josephson tunnelling taking place between them. This contention however seems erroneous for at least two reasons: (1) Recent HRTEM studies of MgB_2 (see the chapter by Y. Zhu et al. in the present volume) have revealed the amorphous region of the grain boundary to be considerably wider, extending up to 50 nm wide, which far exceeds the coherence length, (2) In superconducting quaternary borocarbide YNi_2B_2C, another intermetallic superconductor [22] but with lower T_c of 15.5 K and a larger coherence length of about 6 to 7 nm, the grain boundaries do indeed manifest the weak link effects [23-25]. We have examined this issue by investing the grain boundaries in MgB_2 and YNi_2B_2C by ambient temperature STM / STS techniques at the atomic resolution and our results show that the nature of amorphous region of the grain boundaries in the two intermetallics to be widely different. In the case of MgB_2 the amorphous region, although quite broad, is still metallic, while in the latter it is quasi-insulating. The metallic nature of the grain boundary in MgB_2 gives rise to proximity type junctions between the neighbouring grains with negligible weak link effects. While in YNi_2B_2C the quasi-insulating boundary forms S-I-S junctions with pronounced weak link behaviour. The reason for the metallic nature of the grain

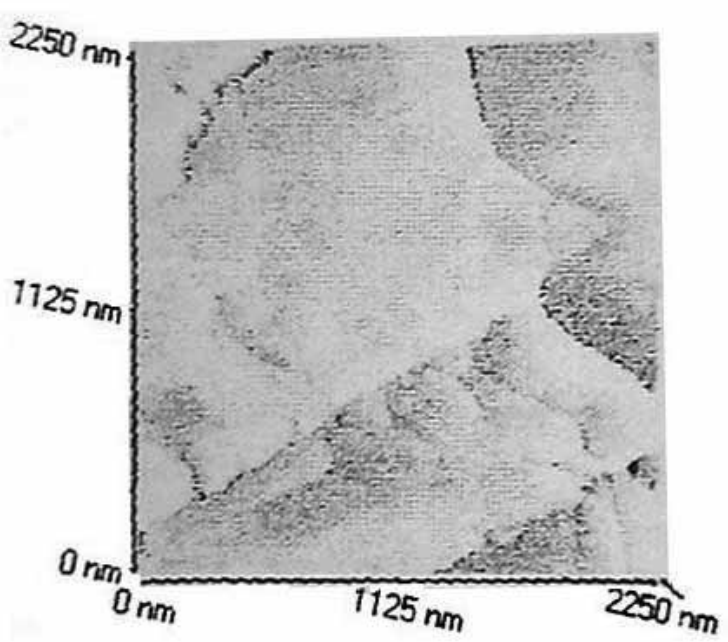

(a)

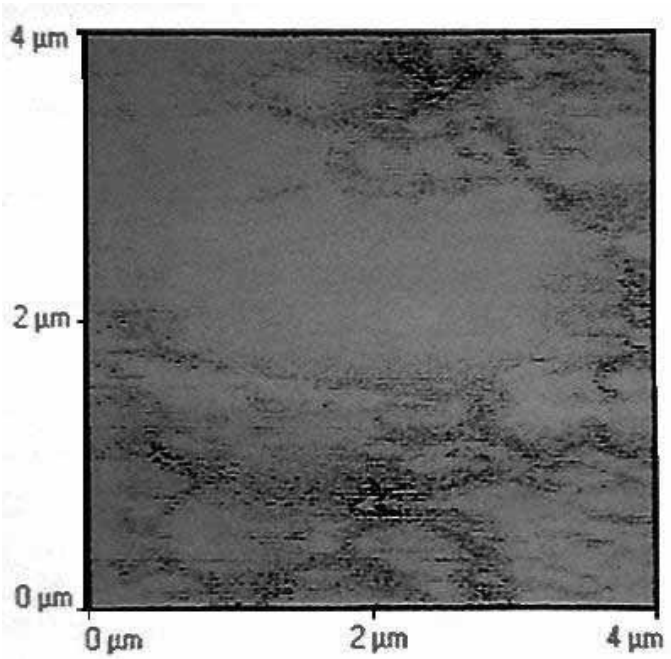

(b)

Fig.3: AFM image, showing (a) grains in hexagonal form (b) zoomed image of a small hexagonal crystal-grain.

boundaries in MgB_2 is believed to arise from its semi metallic type of band structure [14].

STM / STS studies on both intermetallic samples were carried out using a Nanoscope system operating under ambient conditions. All the studies reported here were performed using Pt-Ir tip scanning the surface in constant current mode with zero input filter and using a moderate feedback gain. Once stable and repetitive real images of both grains and grain boundaries were obtained at the atomic level resolution, the instrument was switched into the STS mode and the normalised conduction spectra was obtained within the boundary region as well as inside the grains. The normalised conduction spectra is a measure of local density of states (LDOS) and change sensitively from the characteristic V-shaped metallic type to quasi-insulating type if the scanned layer becomes sufficiently resistive. Thus by mapping the conductance spectra and the way they are changing as one moves away from the centre of the amorphous grain boundary region to the adjoining grains on either side, which are crystallographically ordered, the relative change in the resistive nature of the scanned layer can be determined.

Figs. 4(a,b) and 5(a,b) respectively show the high resolution images of the typical grain boundaries in YNi_2B_2C and MgB_2. The boundary region which is amorphous appears as dark broad band separating crystalline grains on either side which are atomically resolved. In the case of former the amorphous region is around 3 nm wide while in the case of the latter it varies from 5 to 20 nm. HRTEM studies (see Zhu et al. in the present volume) have shown even larger widths of grain boundaries in MgB_2.

In order to estimate the range over which the disorder is spread on either side of the grain boundary, we have carried out a systematic study of the conductance spectra and the way their characteristics change as one moves away from the boundary into the adjoining grains. The results for YNi_2B_2C are shown in Fig. 6. As may be seen, within the grain boundary region, where the atoms are highly disordered, the behaviour of the normalised conductance is markedly distorted from the characteristic metallic-type, indicating quasi-insulating nature of the grain boundary. The normalised conductance close to $V = 0$, which is a measure of LDOS at E_F, is also reduced in comparison, to the metallic type spectra obtained in the middle of the grains. The disturbed region of the grain boundary seems to persist within the adjoining grains up to a distance of about 1.5 nm on either side of the two edges of the boundary region where the spectra observed continue to be distorted. Beyond this distance the metallic-like spectra however seem to get restored on either side of the boundary. These observations indicate that the effective overall width of the grain boundary region in YNi_2B_2C is about 3 nm.

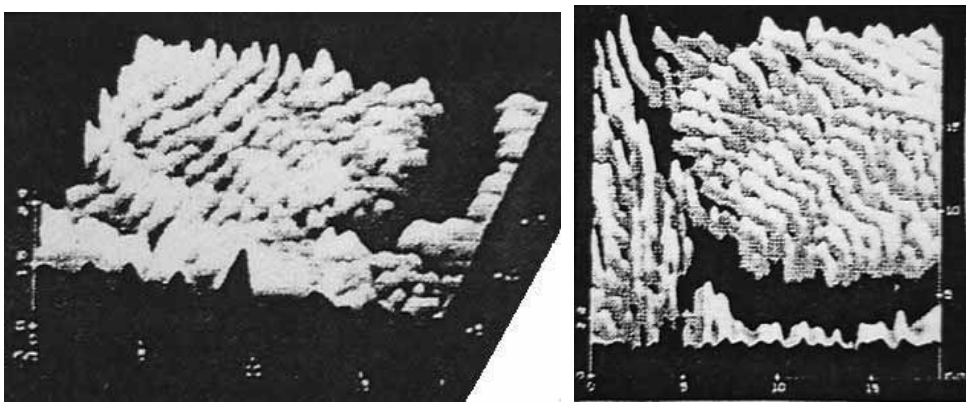

(a) (b)

Fig.4 (a, b): STM images of a grain boundary, 3 nm wide in YNi_2B_2C;
Image in 3D mode at 30° and 60° pitch.

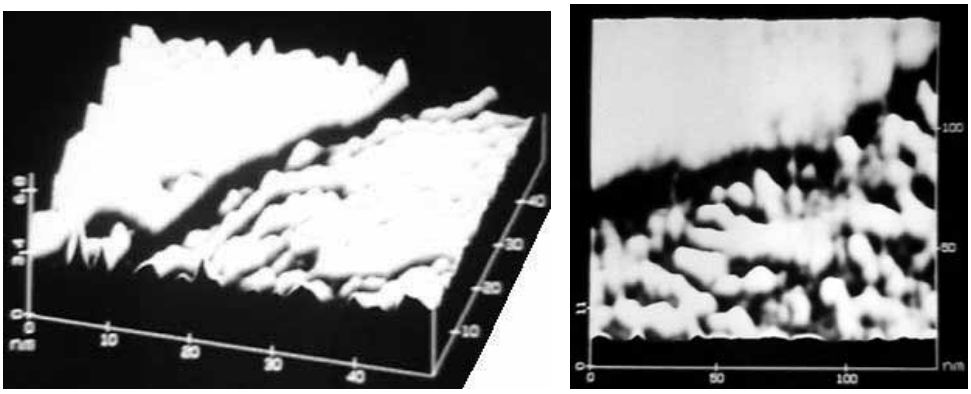

(a) (b)

Fig. 5 (a,b): STM images of a grain boundary, 5 nm to 20 nm wide in MgB_2;
Image in 3D mode at 30° and 60° pitch.

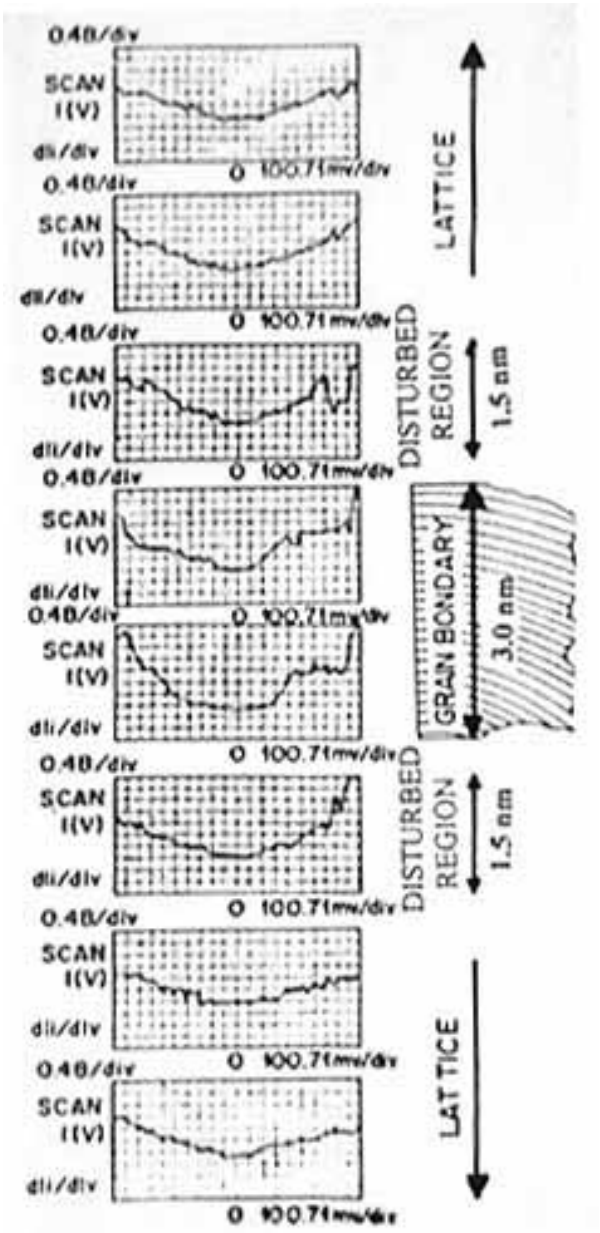

Fig. 6: Conductance spectra obtained within and at different distances away from the grain boundary edges on both sides of the boundary in YNi_2B_2C. Overall boundary region over which the disorder is spread is seen to be 6 nm wide.

The above studies, when repeated for MgB_2, however, yielded unexpected results. The spectra obtained at the centre of the grain boundaries, where the amorphous disorder is expected to be maximum, were far from quasi-insulating and instead were metallic type and indeed did not seem to change significantly from those obtained from the centre of the metallic grains. Fig. 7 depicts a number of normalised conductance spectra obtained at the centres of differently located grain boundaries which are plotted along with a typical spectra observed at the middle of one of the adjoining grains. The normalised conductance near $V = 0$ observed for the boundaries does not seem to vary noticeably from each other and is only marginally lower than for the grain. These results show that the amorphous region of the grain boundary in MgB_2 is quite different from YNi_2B_2C, and instead of being quasi-insulating it is metallic. Consequently, the grains in MgB_2 seem to be mutually coupled through strong proximity or S-N-S type junctions. Such junctions, unlike S-I-S type, in general may have only marginal effect on J_c, except perhaps close to the upper critical

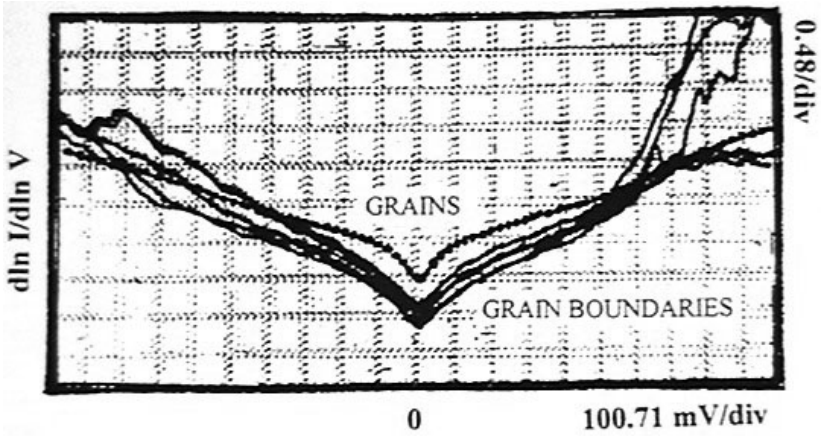

Fig. 7: Conductance spectra obtained within the amorphous regions of various grain boundaries and a representative spectra obtained at the grain interior for the MgB_2 sample.

field H_{c2}. This might explain the negative curvature of $H_{c2}(T)$ near $T = T_c$ observed [2] for MgB_2. Further, the case of low T_c superconductors it has been shown that the proximity junctions can serve as effective pinning centres [26] for realising high J_c values and thus it may not be unlikely that the presence of such junctions might in fact be responsible for the high J_c potential of MgB_2.

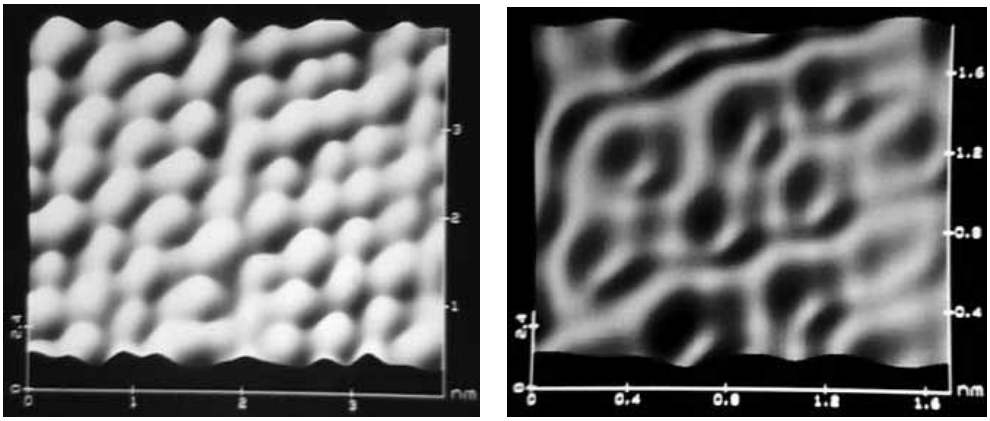

(a) (b)

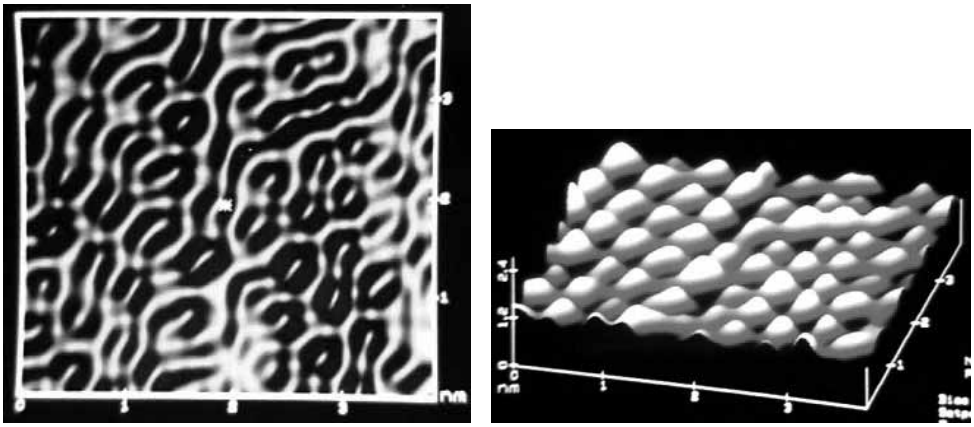

(c) (d)

Fig. 8 (a, b, c, d): Atomically resolved images of the basal plane of MgB_2.

Finally, it is natural to ask why the amorphous region of the grain boundary in MgB_2 is metallic rather than insulating? The answer may be traced to the semi-metallic type of band structure that it is believed to possess [14]. In the case of semi-metals like Bi, Sb, Si and Ge, etc., for example, it is well known that in the amorphous state they exhibit metallic character and show an enhanced conductivity.

4. ATOMICALLY RESOLVED IMAGES OF UNIT CELL AND ION BEAM INDUCED COLUMNAR TYPE DEFECTS IN MgB_2

It has been possible to resolve part of the unit cell of MgB_2 by high resolution STM imaging. Fig. 8 (a, b, c and d) depict the triangular arrangement of Mg atoms (in the form of hexagons with an atom at the centre) forming the basal plane, with the characteristic spacing close to 0.3 nm between the neighbouring Mg atoms, in agreement with the reported lattice parameter of a = 0.308 nm. Interestingly in Fig. 8(c), the boron atoms (appearing as small white circles) may also be seen. Detailed STM studies have further revealed the presence of grown-in defect structures at the atomic level which however remain to be analysed.

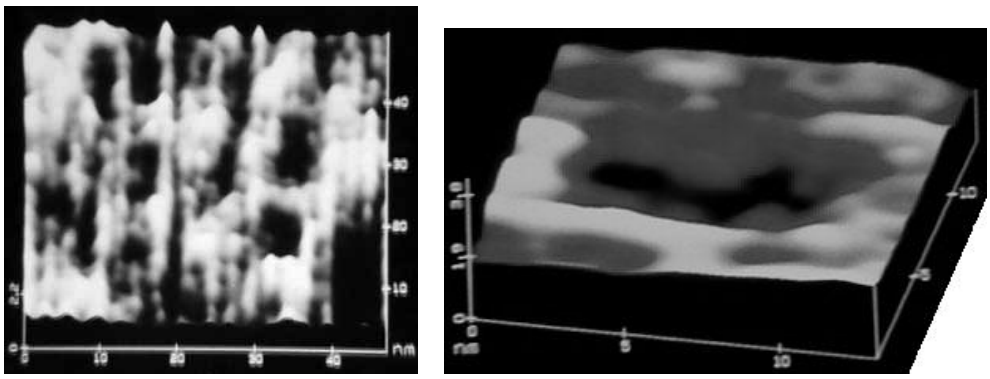

(a) (b)

Fig. 9 (a): Columnar-like defects produced by the beam of Ag ions;
(b) zoomed image of the defect.

We have further investigated the defects produced by the ion beam irradiation. Fig. 9(a) presents sponge-type structure separating columnar-like defects of about 6 to 7 nm diameter produced by 200 MeV beam of Ag ions. The

zoomed image of the defect is shown in Fig. 9(b). These defects seem to comprise of amorphous regions which, from their STS spectra, are found metallic, but perhaps they form non-superconducting regions. Their diameter of 6-7 nm compares reasonably well with the coherence length, and consequently they should provide optimum 'core pinning' of flux vortices and thereby significantly enhance J_c. Their effect on J_c is presently being studied which will form a separate communication to be published elsewhere [27].

5. CONCLUSIONS

While briefly consolidating some of our work, this chapter has addressed the topical macroscopic issue as to why the natural grain boundary in MgB_2 do not show weak link effects? Our STM studies have revealed the grain boundary width, comprising the amorphous regions, in polycrystalline MgB_2 samples to be comparable to or even exceeding the reported value of about 5 nm of the range of coherence. Despite this, the grain boundaries do not cause any serious problem as weak-links. The answer is provided through STS studies of the amorphous region carried out in conjunction with those at the grain interiors. These studies show that the amorphous region is not quasi-insulating as in the quaternary borocarbide where the grain boundaries manifest the S-I-S junction having the weak-link character. Instead, the amorphous region in MgB_2 has the metallic nature, similar to that observed for the grains. Consequently, in MgB_2 the grains are mutually coupled as proximity type junctions, without significantly degrading J_c. These proximity-links between grains, in fact, might effectively serve as pinning centres [26] for flux vortices and account for relatively high J_c values reported for MgB_2. With STM technique it has been possible to resolve part of the unit cell of MgB_2 at the atomic level. Also the columnar-type extended defects have been observed when the sample is subjected to ion beam irradiation. These defects are expected to serve as strong pinning centres to enhance J_c.

Acknowledgement:

The authors thank Prof. R. Nagarajan of TIFR, Mumbai for providing a well characterised sample of YNi_2B_2C for the present study. One of us, (A.V.N) thanks Prof. O.F. de Lima for a stimulating discussion and Prof. F.M. Araujo Moreira for providing hospitality and research facilities at UFSCAR through the funding agency FAPESP and further acknowledges the support of the CSIR emeritus scheme. For the work carried out at Sao Carlos, Brazil, the funding agencies CNPq and FAPESP (Brazil) are thanked.

REFERENCES:

[1] Nagamatsu, J. et al., *Nature* **410** 63 (2001)
[2] de Lima, O.F. et al., *Phys. Rev. Lett.* (in press)
[3] Larbalestier, D.C. et al., *Nature* **410** 186 (2001)
[4] Bugoslavski, Y. et al., *Nature* (in press)
[5] Canfield, P.C. et al., *Phys. Rev. Lett*. **86** 2423 (2001)
[6] Bud'ko, S.L. et al., *Phys. Rev. Lett.* **86** 457 (2001)
[7] Hinks, D.G. et al., *Nature* **411** 457 (2001)
[8] Kremer, R.K. et al., cond-mat / 0102432 (2001)
[9] Wang, Y. et al., cond-mat / 0103181 (2001)
[10] Lorenz, B. et al., cond-mat / 0102264 (2001)
[11] Kotegawa, K. et al., cond-mat / 0102334 (2001)
[12] Rubio-Bollinger, G. et al., *Phys. Rev. Lett.* **86** 5582 (2001)
[13] Kang, W.N. et al., *Science* **292** 1521 (2001)
[14] An, J.M. and Pickett, W.E., cond-mat / 0102391 (2001)
[15] Balashchenko, K.D. et al., cond-mat / 0102290 (2001)
[16] Bascones,E. and Guiena, F., cond-mat / 0103190 (2001)
[17] Imada, M., cond-mat / 0103006 (2001)
[18] Voelker, K. et al., cond-mat / 0103082 (2001)
[19] Hirsch, J.E. and Marsinglio,F., cond-mat / 0102479
[20] Baskaran, G., cond-mat / 0103308 (2001)
[21] Dimos, D. et al., *Phys. Rev*. **B41** 4038 (1990)
[22] Gupta, L.C., *Phil. Mag.* **B77** 717 (1998)
[23] Khare, N. et al., *Appl. Phys. Lett.* **69** 1483 (1996)
[24] Khare, N. et al., *Physica* **C316** 257 (1999)
[25] Rao, T.V.C. et al., *Physica* **C249** 271 (1995)
[26] Kramer, E.J. and Frayhardt, H.C., *J. Appl. Phys.* **51** 4930 (1980)
[27] Narayan, H. et al., *to be published.*